Metal–Metal Interactions

DOI: 10.1002/anie.200903895

Two-Dimensional Triangular and Square Heterometallic Clusters: Influence of the Closed-Shell d^{10} Electronic Configuration**

Sabrina Sculfort, Pierre Croizat, Abdelatif Messaoudi, Marc Bénard, Marie-Madeleine Rohmer, Richard Welter, and Pierre Braunstein**

Dedicated to Professor Michael Veith on the occasion of his 65th birthday

The study of metal–metal bonding in molecules is at the crossroads of the development of the interface between chemical bonding, cooperative reactivity, modeling of the interactions between organic ligands and metal surfaces (particularly in the case of 2D metal cores), multicenter catalysis, and metal-rich nanomaterials.[1] It is now well recognized that small gold particles and surfaces display unique electronic properties[2] and catalytic reactivity that were not anticipated for such a noble metal.[3] The development of synthetic approaches towards organized, heterometallic 2D structures is particularly attractive because of the increased challenges compared to homometallic structures and their possible relevance to modeling of interactions between substrates and alloy surfaces. The synthesis of the first heterometallic complexes containing a metal–metal bond between a Group 11 d^{10} ion M and another transition metal M′[4] triggered considerable interest in the synthesis and study of complexes and clusters with M–M′ bonds.[5] In some cases, there is structural evidence for additional $d^{10}\cdots d^{10}$ M–M inter- or intramolecular interactions, which cannot be considered as conventional covalent or dative bonds and are of major current interest from experimental and theoretical points of view.[6] When no ligand is coordinated to the d^{10} ions (bare ions), they can only be involved in metal–metal bonding and may for example, bridge across one or two metal–metal bonds, as in triangular or bow-tie clusters, respectively, or cap one or two triangular metal faces, serving then as connector between metal polyhedra to form discrete or oligomeric species.[1,5a] In heterometallic complexes containing a single d^{10} ion, only intermolecular $d^{10}\cdots d^{10}$ interactions are possible, and it is often difficult to assess their contribution to the overall structure versus that of packing forces. Thus, we are interested in studying intramolecular $d^{10}\cdots d^{10}$ interactions, in particular of the heterometallic type which are rarer than the homometallic type.[7] We report here a series of heterometallic clusters of general formula $[MMoCp(CO)_3]_n$ (Cp = η^5-C_5H_5; M = Cu, $n = 3$; M = Ag or Au, $n = 4$), the nuclearity and structure of which critically depend on the nature of the d^{10} ions. Experimental and theoretical data suggest that $d^{10}\cdots d^{10}$ interactions are responsible for the observed differences.

The reaction of $[Cu(NCMe)_4]PF_6$ with Na·**1**·2DME in THF afforded the yellow cluster $[Cu_3\{MoCp(CO)_3\}_3]$ (**2**; Figure 1a).[8] Its metal skeleton contains a Cu^I_3 triangle whose edges are bridged by the metalloligand $\{MoCp(CO)_3\}$ and which is inscribed within an almost equilateral Mo_3 triangle (Mo1···Mo2 = 5.269(1), Mo2···Mo3 = 5.269(1), Mo1···Mo3 = 5.297(1) Å for **2**·0.5C_4H_8O). Accordingly, this Cu_3Mo_3 raft-type cluster has a triangular metal core of frequency 2 (ν_2 triangle, Figure 1b).

The Cu–Mo distances are similar to those found in the literature for such bonds (median value from CCSD November 2008: 2.705 Å, $\sigma = 0.11$ Å for 378 samples). Two other crystalline modifications of this cluster have been structurally characterized, with similar bonding parameters (see Supporting Information). Although the linear Mo-Cu-Mo arrangements are as expected for a two-coordinate Cu^I center, the relatively short Cu–Cu distances suggest additional bonding.

The reaction of $AgBF_4$ with Na·**1**·2DME in THF afforded the yellow cluster $[Ag_4\{MoCp(CO)_3\}_3]$ (**3**; Figure 2a).[8] Each Ag–Ag edge of the distorted silver square is bridged by a μ-$\{MoCp(CO)_3\}$ fragment in such a way that the inner Ag_4 polygon is inscribed within a distorted Mo_4 rhombus (Mo1···Mo2 5.638(1), Mo1′···Mo2 5.475(1) Å), which results in a distorted ν_2-square-type structure for the Ag_4Mo_4 metal core (Figure 2b). The molybdenum atoms are not coplanar with the inner silver square, since a slight tetrahedral distortion around the silver centers results in two opposite Mo atoms being located on the same side of the Ag_4 mean plane (Figure 2b).

The Ag–Mo distances are similar to the values reported for such bonds (median value from CCSD November 2008: 2.961 Å, $\sigma = 0.07$ Å for 85 samples). The almost linear Mo-Ag-Mo arrangements are as expected for two-coordinate Ag^I

---

[*] Dr. M. Bénard, Dr. M.-M. Rohmer
Laboratoire de Chimie Quantique
Institut de Chimie (UMR 7177 CNRS), Université de Strasbourg
4 rue Blaise Pascal, 67070 Strasbourg (France)
E-mail: benard@chimie.u-strasbg.fr

S. Sculfort, P. Croizat, A. Messaoudi, Dr. P. Braunstein
Laboratoire de Chimie de Coordination
Institut de Chimie (UMR 7177 CNRS), Université de Strasbourg
4 rue Blaise Pascal, 67070 Strasbourg (France)
Fax: (+33) 3-6885-1322
E-mail: braunstein@chimie.u-strasbg.fr

Prof. R. Welter
Laboratoire DECOMET, Institut de Chimie (UMR 7177 CNRS)
Université de Strasbourg
4 rue Blaise Pascal, 67070 Strasbourg (France)

[**] Support from the CNRS, the Ministère de l'Enseignement Supérieur et de la Recherche, the DFH/UFA, the DFG International Research Training Group GRK532, the IDRIS and CINES computer centers, and the Agence Nationale de la Recherche (ANR-06-BLAN-410) is gratefully acknowledged.

Supporting information for this article is available on the WWW under http://dx.doi.org/10.1002/anie.200903895.

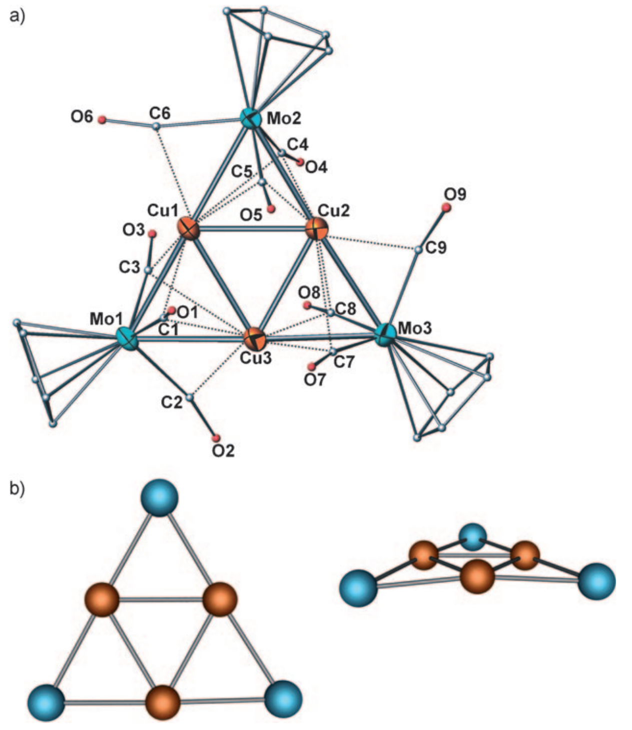

Figure 1. a) View of the molecular structure of **2** in **2**·0.5 C_4H_8O. Selected bond lengths [Å] and angles [°]: Cu1–Cu2 2.6211(13), Cu2–Cu3 2.6167(13), Cu1–Cu3 2.6594(13), Mo1–Cu1 2.6526(10), Mo2–Cu1 2.6194(10), Mo2–Cu2 2.6477(11), Mo3–Cu2 2.6215(12), Mo1–Cu3 2.6439(11), Mo3–Cu3 2.6685(11); Cu2-Cu1-Cu3 59.41(3), Cu1-Cu2-Cu3 61.03(4), Cu1-Cu3-Cu2 59.57(3), Mo1-Cu1-Mo2 175.92(5), Mo2-Cu2-Mo3 177.87(5), Mo1-Cu3-Mo3 171.25(5). b) Views of the metal core of **2** in **2**·0.5 C_4H_8O.

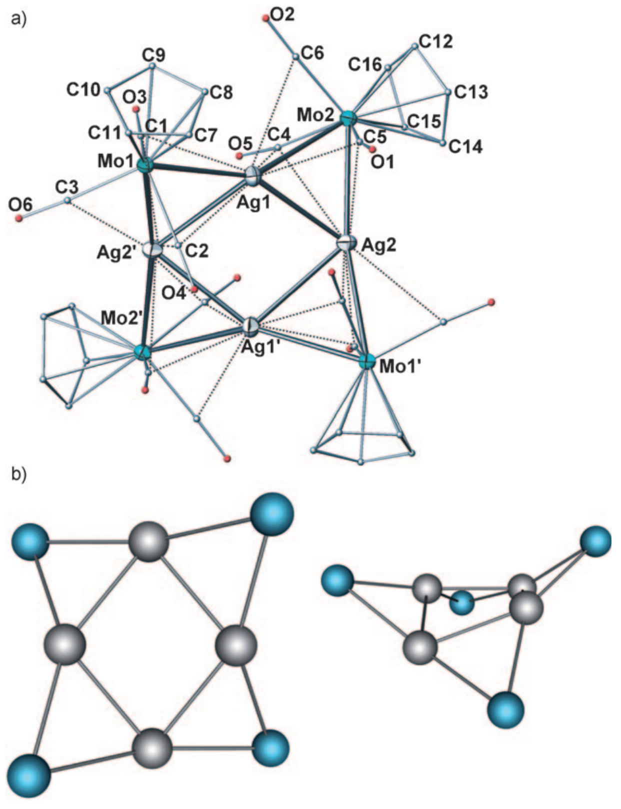

Figure 2. a) View of the molecular structure of **3**. Selected bond lengths [Å] and angles [°]: Ag1–Ag2 2.8408(9), Ag1–Ag2′ 2.8999(9), Ag1⋯Ag1′ 3.5314(11), Ag2⋯Ag2′ 4.4051(10), Mo1–Ag1 2.8115(9), Mo2–Ag1 2.8868(9), Mo1′–Ag2 2.8750(10), Mo2–Ag2 2.8216(10); Ag2-Ag1-Ag2′ 100.23(3), Ag1-Ag2-Ag1′ 75.92(3), Mo1-Ag1-Mo2 147.80(3), Mo1′-Ag2-Mo2 163.56(3). b) Views of the metal core of **3**.

centers. Like the Cu–Cu distances in **2**, the relatively short Ag–Ag distances suggest additional bonding, consistent with inward bending of the Mo-Ag-Mo chains, which is more pronounced at Ag1.

The reaction of Na·**1**·2DME in toluene with $NEt_4[AuBr_2]$ in acetone at −40 °C, in a 1:1 ratio, led to instant formation of temperature-sensitive red cluster $[Au_4\{MoCp(CO)_3\}_4]$ (**4**; Figure 3a).[8] Its Au_4Mo_4 metal core contains a tetragold square, and each Au–Au edge is bridged by a μ-$\{MoCp(CO)_3\}$ fragment. Consequently, the inner Au_4 square is inscribed within a distorted Mo_4 square (Mo⋯Mo 5.438(1)–5.535(1) Å; ν_2-square structure for the Au_4Mo_4 metal core shown in Figure 3b). The Mo atoms are not coplanar with the gold square and, like in **3**, a slight tetrahedral distortion around the gold centers means that two opposite molybdenum atoms are located on the same side of the Au_4 plane (Figure 3b). The Au–Mo distances are in agreement with the literature values reported for such bonds (median value from CCSD November 2008: 2.803 Å, $\sigma = 0.12$ Å for 76 samples). The bonding situation of the CO ligands in clusters **2**–**4** is discussed in the Supporting Information.

Whereas the average M–M distances in **2**–**4** (Cu–Cu 2.632(1), Ag–Ag 2.870(1), Au–Au 2.774(1) Å) are close to the respective sums of the metal atomic radii (2.556, 2.890, and 2.884 Å[9a]) and covalent radii (2.64(4), 2.90(5), and 2.72(6) Å[9b]), they are significantly shorter than the sums of the van der Waals radii (2.80, 3.44, 3.32, respectively),[9c] and the respective experimental values (median values from CCSD November 2008: 2.701 Å, $\sigma = 0.21$ Å for 3946 samples; 3.016 Å, $\sigma = 0.20$ Å for 3343 samples; and 2.918 Å, $\sigma = 0.19$ Å for 2940 samples). This, together with the average inward bending of the Mo-M-Mo chains in the ν_2 squares, which is more pronounced in **4** than in **3**, strongly suggests the existence of attractive $d^{10}\cdots d^{10}$ interactions.[6] The question arises to what extent the nature of the d^{10} ion and of the $d^{10}\cdots d^{10}$ interactions determines the preference for a ν_2-triangular $(MM')_3$ or a ν_2-square $(MM')_4$ core geometry in such mixed-metal clusters.

We carried out DFT/B3LYP calculations[10] with the Gaussian 03 software suite[11] to inquire into the preference of Cu^I to form triangular clusters whereas the heavier homologues give rise to square-like clusters. Both types of clusters were therefore modeled with Cu, Ag, and Au cores. The geometry observed for **2** was modeled by a trimer with C_{3v} symmetry, reduced to C_s in the calculations. For the tetramer, the structure with lowest energy was obtained, whatever the metal, for a geometry displaying S_4 molecular symmetry and strongly reminiscent of the structures observed for **3** and **4**, although the out-of-plane deformation of the metal framework could not be reproduced by geometry optimization. For both the triangular and square complexes,

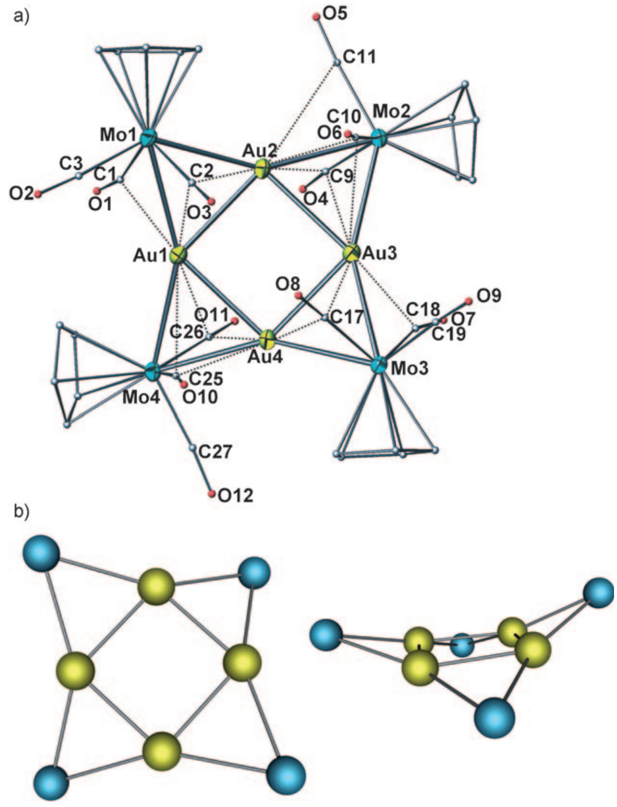

Figure 3. a) View of the molecular structure of **4** in **4**$\cdot$$C_7H_8$. Selected bond lengths [Å] and angles [°]: Au1–Au2 2.7417(8), Au2–Au3 2.8030(9), Au3–Au4 2.7512(8), Au4–Au1 2.7995(9), Au1$\cdots$Au3 3.9391(11), Au2$\cdots$Au4 3.9041(10), Mo1–Au1 2.8527(12), Mo4–Au1 2.8243(12), Mo1–Au2 2.8054(12), Mo2–Au2 2.8114(11), Mo2–Au3 2.7975(11), Mo3–Au3 2.8259(12), Mo3–Au4 2.8244(12), Mo4–Au4 2.8077(11); Au2-Au1-Au4 89.58(2), Au1-Au2-Au3 90.53(2), Au2-Au3-Au4 89.32(2), Au3-Au4-Au1 90.41(2), Mo1-Au1-Mo4 154.29(3), Mo1-Au2-Mo2 150.99(3), Mo2-Au3-Mo3 153.87(3), Mo3-Au4-Mo4 152.18(3). b) Views of the metal core of **4** in **4**$\cdot$$C_7H_8$.

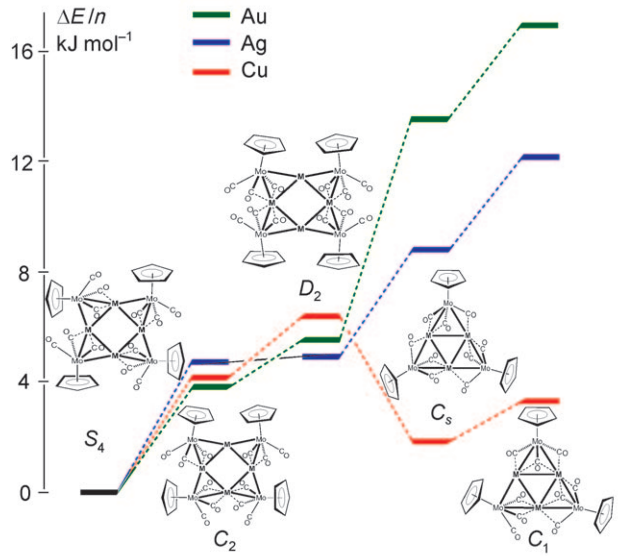

Figure 4. Representation of the relative energies computed for various possible structures of $[M\{MoCp(CO)_3\}]_n$ (M = Cu, Ag, Au; n = 3, 4) and reduced to a single hypothetical monomer (n = 1). For each metal M, the zero-energy level of the monomer corresponds to the square structure of S_4 symmetry.

distinct starting geometries, differing in the relative orientations of the $\{MoCp(CO)_3\}$ fragments and in the molecular symmetry (Figure 4), yielded separate local minima, although higher in energy. To compare the relative stabilities of the trimers with those of the tetramers, the total energy E optimized for a given cluster was reduced to the averaged energy of a hypothetical $M[MoCp(CO)_3]$ monomer as E/n ($n = 3$ or 4). Values of E/n obtained for all five considered cluster forms of Cu, Ag and Au, together with the corresponding Cartesian coordinates are displayed in the Supporting Information. Figure 4 shows the relative averaged energies $\Delta E/n$ obtained for the three coinage metals with respect to the geometry optimized starting from the structure of the tetramer with S_4 symmetry, which was the most stable whatever the metal.

All values of $\Delta E/n$ are small, that is, less than 7, 12, and 18 kJ mol^{-1} for Cu, Ag, and Au, respectively. The square-like structure with C_2 symmetry, for instance, had $\Delta E/n \approx +4$ kJ mol^{-1}, whatever the metal. It is therefore not ruled out that clusters closely related to **3** and **4** could exist with slightly different geometries of the $\{MoCp(CO)_3\}$ moieties, depending on intra- or intermolecular interactions. Similarly, the configuration of the Cu trimer with C_1 symmetry is separated from the triangular form of lowest energy by no more than 1.4 kJ mol^{-1} (Figure 4).

The most important trend, however, concerns the values of $\Delta E/n$ separating the trimers from the tetramers. Even though the lowest energy tetramer is always calculated to be more stable than the lowest trimer, the gap is particularly small for Cu (1.9 kJ mol^{-1}), and remains compatible with stabilization of the smallest cluster, given the possible influence of entropy factors. Then, the $\Delta E/n$ gap increases to 8.7 kJ mol^{-1} for silver and culminates at 13.5 kJ mol^{-1} for Au, in agreement with the observed preference of these two metals for square-like clusters.

The origin of these differences could be sought in steric repulsion between the $\{MoCp(CO)_3\}$ moieties. To check this hypothesis, single-point calculations were carried out on the 15 clusters of Figure 4 after removing the coinage-metal core. To avoid electrostatic bias, an Mo^I oxidation state was assumed in each fragment. Figure 5 displays the values of $\Delta E/n = E/n - E_{opt}$, where E/n represents the energy of the $\{MoCp(CO)_3\}$ fragment averaged from the computed energy of a $[MoCp(CO)_3]_n$ cluster, and E_{opt} is the reference energy of an optimized $\{Mo^ICp(CO)_3\}$ fragment. It shows that the average destabilization of the $\{MoCp(CO)_3\}$ moieties is almost independent of the coinage-metal core for the square forms, which are expected to be more sensitive to ligand crowding. The $\{MoCp(CO)_3\}$ moiety extracted from copper triangle **2** with C_s symmetry displays surprising destabilization (Figure 5). A closer analysis shows that the latter is not due to interfragment repulsion, but to deformation of the $\{Mo(CO)_3\}$ tripods induced by semibridging coordination of the carbonyl ligands. Among the 15 inves-

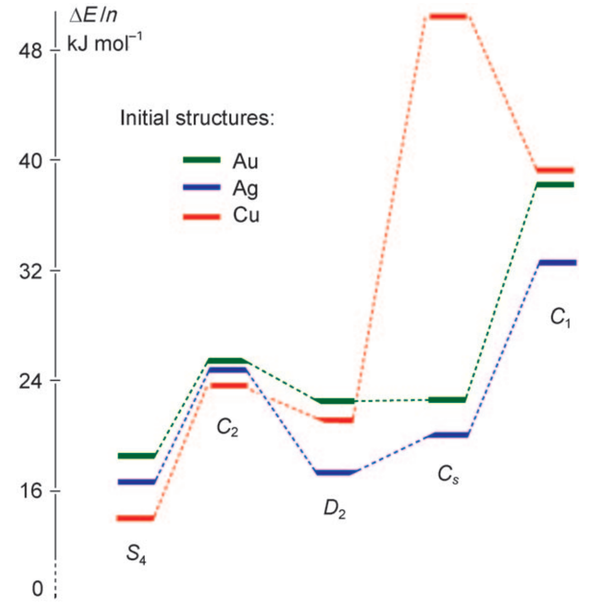

Figure 5. Averaged relative energies of $\{MoCp(CO)_3\}$ fragments obtained from single-point calculations on the various structures of $[\{Mo^{I}Cp(CO)_3\}]_n$ ($n = 3, 4$) extracted from $[M\{MoCp(CO)_3\}]_n$ (M = Cu, Ag, Au; Figure 4) and compared with an isolated $\{Mo^{I}Cp(CO)_3\}$ fragment with optimized geometry.

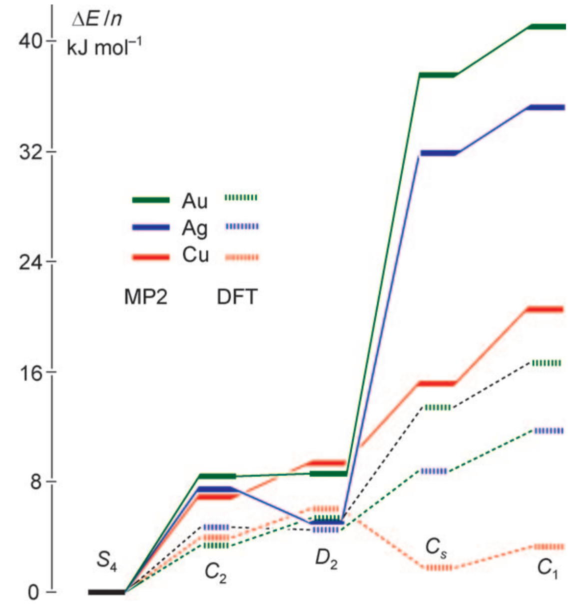

Figure 6. Averaged relative energies of $M[MoCp(CO)_3]$ monomers obtained from single-point MP2 calculations carried out on the clusters displayed in Figure 4 and using the DFT-optimized structures (solid lines). The DFT results are indicated by dotted lines. The origin of the energy scale is the same as in Figure 4.

tigated clusters, the model of **2** is the only one in which all carbonyl ligands are involved in strong semi-bridging contacts with the copper core.

In the three square clusters of S_4 symmetry, as in the Au and Ag triangles with C_s symmetry, only two carbonyl ligands out of three are engaged in semibridging interactions, which gives the $\{Mo(CO)_3\}$ tripod sufficient flexibility.[12] The results summarized in Figures 4 and 5 suggest better capability of Cu^{I} to retrodonate electrons toward the CO π^* orbitals and rationalize the coordination modes observed for **2**, **3**, and **4** (Figure 1 a–3 a).[13] However, this coordination mode affects each of the $\{MoCp(CO)_3\}$ fragments individually in their interaction with the two closest coinage-metal atoms. Clearly, the difference in the metal affinities toward CO π^* MOs, and in a more general way the results displayed in Figure 5, do not provide indications why Cu should prefer the triangle and Ag and Au, the square.

Nevertheless, the sequence of relative stabilities displayed in Figure 4 is reminiscent of metallophilic trends, and it is therefore tempting to correlate the increase of the M_3/M_4 gap while descending the Periodic Table with the strengthening of $d^{10}\cdots d^{10}$ interactions specific to tetramers, that is, those connecting the coinage metals along the diagonals of the M_4 squares. Even though these diagonal distances approach 4 Å in Au cluster **4**, the aurophilic interaction has been shown to slowly decrease with increasing Au···Au separation and still provide an appreciable stabilizing contribution in this range of distances.[6a, 14] Since the DFT/B3LYP approach is known to underestimate these interactions, the results of Figure 4 were refined with single-point MP2 calculations, which are expected to provide a more reliable account of the dispersion part of the metallophilic interactions.[6,14] The MP2 results (Figure 6) indeed find the triangles to be significantly destabilized with respect to all square structures, whatever the metal.

Moreover, the destabilization obtained with MP2 for the triangular forms of the Ag and Au complexes is clearly increased with respect to the DFT results. These results strongly substantiate the hypothesis of diagonal and/or multicenter metallophilic interactions stabilizing the square-like clusters of Ag and Au. However, the present MP2 results fail to account for the observed triangular form of Cu complex **2**.

The only ν_2-triangular clusters comparable to **2** have Fe_3Cu_3[15] and Os_3Cu_3[16] cores, and only four ν_2-square $M_4M'_4$ clusters have M–M distances in the central group 11 M_4 square or rhombus shorter than 3.4 Å. Two of them feature Cu^{I} or Ag^{I} squares with edge-bridging μ-$\{Co(CO)_4\}$ metalloligands,[17] and the other two contain Ag^{I} or Au^{I} squares with edge-bridging μ-$\{Fe(CO)_4\}$ metalloligands.[18] However, their mean Ag–Ag (3.021[17b] and 3.149 Å[18a]) and Au–Au distances (2.902 Å)[18b] are longer than in **3** and **4**, respectively.

Complexes **2**–**4** form a unique series of oligomeric clusters of type $\{M[m]\}_n$ (M = Cu, Ag, and Au) containing the same bridging metalloligand [m], and thus provide comparative structural data relevant to a better evaluation of the contribution of $d^{10}\cdots d^{10}$ interactions in structural chemistry. Theoretical calculations suggest that formation of squares instead of triangles in the case of Au and Ag could be favored by diagonal Au···Au and Ag···Ag interactions, respectively.

Received: July 16, 2009
Published online: October 12, 2009

Keywords: coinage metals · density functional calculations · heterometallic clusters · metal–metal interactions · metallophilic interactions

[1] See for example, a) *Metal Clusters in Chemistry* (Eds.: P. Braunstein, L. A. Oro, P. R. Raithby), Wiley-VCH, Weinheim, **1999**; b) *Catalysis by Di- and Polynuclear Metal Cluster Complexes* (Eds.: R. D. Adams, F. A. Cotton), Wiley-VCH, New York, **1998**; c) *The Chemistry of Metal Cluster Complexes* (Eds.: D. F. Shriver, H. D. Kaesz, R. D. Adams), VCH, New York, **1990**.

[2] See, for example, G. Schmid, *Chem. Soc. Rev.* **2008**, *37*, 1909–1930, and the articles in this special issue dedicated to "Gold, Chemistry, Materials and Catalysis".

[3] G. J. Hutchings, *Dalton Trans.* **2008**, 5523, and references therein.

[4] C. E. Coffey, J. Lewis, R. S. Nyholm, *J. Chem. Soc.* **1964**, 1741–1749.

[5] a) I. D. Salter in *Comprehensive Organometallic Chemistry II*, *Vol. 10* (Eds.: E. W. Abel, F. G. A. Stone, G. Wilkinson), Pergamon, New York, **1995**, p. 255; b) M. J. Chetcuti in *Comprehensive Organometallic Chemistry II*, *Vol. 10* (Eds.: E. W. Abel, F. G. A. Stone, G. Wilkinson), Pergamon, New York, **1995**, p. 23; c) V. Ritleng, M. J. Chetcuti, *Chem. Rev.* **2007**, *107*, 797–858, and references therein.

[6] a) P. Pyykkö, *Chem. Rev.* **1997**, *97*, 597–636; b) P. Pyykkö, *Angew. Chem.* **2002**, *114*, 3723–3728; *Angew. Chem. Int. Ed.* **2002**, *41*, 3573–3578; c) P. Pyykkö, *Angew. Chem.* **2004**, *116*, 4512–4557; *Angew. Chem. Int. Ed.* **2004**, *43*, 4412–4456; d) M. A. Carvajal, S. Alvarez, J. J. Novoa, *Chem. Eur. J.* **2004**, *10*, 2117–2132; e) P. Pyykkö, *Inorg. Chim. Acta* **2005**, *358*, 4113–4130; f) P. Pyykkö, *Chem. Soc. Rev.* **2008**, *37*, 1967–1997.

[7] M. Bénard, U. Bodensieck, P. Braunstein, M. Knorr, M. Strampfer, C. Strohmann, *Angew. Chem.* **1997**, *109*, 2890–2893; *Angew. Chem. Int. Ed. Engl.* **1997**, *36*, 2758–2761; W. Schuh, P. Braunstein, M. Bénard, M.-M. Rohmer, R. Welter, *Angew. Chem.* **2003**, *115*, 2211–2214; *Angew. Chem. Int. Ed.* **2003**, *42*, 2161–2164; W. Schuh, P. Braunstein, M. Bénard, M.-M. Rohmer, R. Welter, *J. Am. Chem. Soc.* **2005**, *127*, 10250–10258.

[8] CCDC 720822, 720823, 720824, 720825, 720826 contain the supplementary crystallographic data for this paper. These data can be obtained free of charge from The Cambridge Crystallographic Data Centre via www.ccdc.cam.ac.uk/data_request/cif.

[9] a) A. F. Holleman, E. Wiberg, *Lehrbuch der Anorganischen Chemie*, 91st ed., W. de Gruyter, Berlin, **1985**; b) B. Cordero, V. Gómez, A. E. Platero-Prats, M. Revés, J. Echeverria, E. Cremades, F. Rarragán, S. Alvarez, *Dalton Trans.* **2008**, 2832–2838; c) A. Bondi, *J. Phys. Chem.* **1964**, *68*, 441–451.

[10] All calculations were carried out with the Gaussian 03 software suite.[11] Stuttgart–Dresden relativistic electron core potentials were used for all metals. The valence shell of the metal atoms, namely, the *n*spd and $(n+1)$s shells, were described by means of triple-ζ Gaussian basis sets, supplemented with diffuse p functions and with one f-type polarization function (G. Frenking et al., *Chem. Phys. Lett.* **1993**, *208*, 111–114). In the DFT/B3LYP calculations, C, O, and H atoms were described by all-electron 6-311G** basis sets. The single-point MP2 calculations were carried out on the geometry optimized at the DFT level. The same basis sets were used for the metal atoms, but the other atoms were described with smaller, LANL2DZ basis sets.

[11] Gaussian 03, Revision B.05, M. J. Frisch et al., Gaussian, Inc., Pittsburgh, PA, **2003**.

[12] In the triangular clusters with C_1 symmetry, 11 out of 12 carbonyl ligands display a semibridging bonding mode. At variance with the case of the C_s triangles, this coordination mode is retained for all three coinage metals, and thus gives rise to a large average deformation energy for the $\{MoCp(CO)_3\}$ fragments (Figure 5). All computed structures are displayed in the Supporting Information.

[13] A coordination mode in which all carbonyl ligands are engaged in semibridging bonds with copper was designed in square-like model complexes of Cu with D_2 and S_4 symmetries. The 12 semibridging interactions subsisted after geometry optimization, and the total bond energies differed by less than 1 kJ mol^{-1} from that of the most stable square structure with S_4 symmetry and nine semibridging interactions. Similar configurations optimized with Ag and Au are however significantly destabilized.

[14] P. Pyykkö, J. Li, N. Runeberg, *Chem. Phys. Lett.* **1994**, *218*, 133–138.

[15] G. Doyle, K. A. Eriksen, D. Van Engen, *J. Am. Chem. Soc.* **1986**, *108*, 445–451.

[16] T. H. Lemmen, J. C. Huffman, K. G. Caulton, *Angew. Chem.* **1986**, *98*, 267–268; *Angew. Chem. Int. Ed. Engl.* **1986**, *25*, 262–264.

[17] a) P. Klüfers, *Angew. Chem.* **1984**, *96*, 288–290; *Angew. Chem. Int. Ed. Engl.* **1984**, *23*, 307–308; b) P. Klüfers, *Z. Kristallogr.* **1984**, *166*, 143–151.

[18] a) V. G. Albano, F. Azzaroni, M. C. Iapalucci, G. Longoni, M. Monari, S. Mulley, D. M. Proserpio, A. Sironi, *Inorg. Chem.* **1994**, *33*, 5320–5328; b) V. G. Albano, F. Calderoni, M. C. Iapalucci, G. Longoni, M. Monari, *J. Chem. Soc. Chem. Commun.* **1995**, 433–434.